PNAS RESEARCH ARTICLE | GENETICS

Integrated regulation of dopaminergic and epigenetic effectors of neuroprotection in Parkinson's disease models

J. Brucker Nourse Jr.[a], Shannon N. Russell[a], Nathan A. Moniz[a], Kylie Peter[a], Lena M. Seyfarth[a], Madison Scott[b], Han-A Park[b,c,d], Kim A. Caldwell[a,c,d,e], and Guy A. Caldwell[a,d,e,1]

Edited by Hugo Bellen, Baylor College of Medicine, Houston, TX; received June 22, 2022; accepted January 5, 2023

Whole-exome sequencing of Parkinson's disease (PD) patient DNA identified single-nucleotide polymorphisms (SNPs) in the tyrosine nonreceptor kinase-2 (*TNK2*) gene. Although this kinase had a previously demonstrated activity in preventing the endocytosis of the dopamine reuptake transporter (DAT), a causal role for TNK2-associated dysfunction in PD remains unresolved. We postulated the dopaminergic neurodegeneration resulting from patient-associated variants in *TNK2* were a consequence of aberrant or prolonged TNK2 overactivity, the latter being a failure in TNK2 degradation by an E3 ubiquitin ligase, neuronal precursor cell-expressed developmentally down-regulated-4 (NEDD4). Interestingly, systemic RNA interference protein-3 (SID-3) is the sole TNK2 ortholog in the nematode *Caenorhabditis elegans*, where it is an established effector of epigenetic gene silencing mediated through the dsRNA-transporter, SID-1. We hypothesized that TNK2/SID-3 represents a node of integrated dopaminergic and epigenetic signaling essential to neuronal homeostasis. Use of a TNK2 inhibitor (AIM-100) or a NEDD4 activator [N-aryl benzimidazole 2 (NAB2)] in bioassays for either dopamine- or dsRNA-uptake into worm dopaminergic neurons revealed that *sid-3* mutants displayed robust neuroprotection from 6-hydroxydopamine (6-OHDA) exposures, as did AIM-100 or NAB2-treated wild-type animals. Furthermore, NEDD4 activation by NAB2 in rat primary neurons correlated to a reduction in TNK2 levels and the attenuation of 6-OHDA neurotoxicity. CRISPR-edited nematodes engineered to endogenously express SID-3 variants analogous to *TNK2* PD-associated SNPs exhibited enhanced susceptibility to dopaminergic neurodegeneration and circumvented the RNAi resistance characteristic of SID-3 dysfunction. This research exemplifies a molecular etiology for PD whereby dopaminergic and epigenetic signaling are coordinately regulated to confer susceptibility or resilience to neurodegeneration.

dopamine | neuroprotection | *C. elegans* | Parkinson's disease | RNA

Parkinson's disease (PD) is a neurodegenerative disease associated with the progressive degeneration of dopaminergic neurons in the *substantia nigra*. The significant loss of these neurons results in an attenuated dopaminergic signal, ultimately manifesting into the characteristic symptoms of PD including rigidity and resting tremors. While advances in genome sequencing have expanded the lists of genes and cellular pathways associated with PD, the search to identify a successful disease-modifying therapeutic target remains to be fulfilled. Among these expanding genomic datasets was a whole-exome sequencing (WES) study that revealed the tyrosine nonreceptor kinase-2 (*TNK2*) gene, encoding the human TNK2 protein, to be mutated in a group of patients with familial PD (1).

Human TNK2 (also referred to as ACK1) is involved in several cellular pathways and is highly expressed in presynaptic vesicles of neurons in the mammalian brain (2, 3), where it functions in the regulation of clathrin-dependent endocytosis of the dopamine transporter (DAT) (4). While the precise mechanism by which TNK2 modulates clathrin-dependent endocytosis is unknown, TNK2 possesses a clathrin-heavy chain domain and has been shown to interact with established regulators of vesicular dynamics including clathrin, adaptor protein-2, and sortin nexin-9 (5). TNK2 is activated by GTP-bound CDC42 phosphorylation, and conversely, is marked for protein degradation by the E3 ubiquitin ligase NEDD4 (neuronal precursor cell-expressed developmentally down-regulated-4) (6). Furthermore, TNK2 specifically interacts with DAT at the neuronal plasma membrane, directly modulating dopamine reuptake from the synapse (7). Our interest in TNK2 was piqued by having previously reported the discovery of a small molecule activator of NEDD4 ubiquitin ligase activity, N-aryl benzimidazole 2 (NAB2), that exhibited potent and selective neuroprotection from dopaminergic neurodegeneration across multiple PD models including in the nematode *Caenorhabditis elegans* and

Significance

The progressive loss of dopaminergic neurons is a pathological hallmark of Parkinson's disease (PD). Distinctions between resilience or susceptibility to neurodegeneration in PD are a combined consequence of genetic predisposition and environmental factors, the latter often manifesting as changes in gene expression that are coordinately controlled by small RNA molecules. This research reveals a functional convergence of proteins that modulate uptake of both dopamine and small RNAs, as a regulatory intersection for the integrated control of dopaminergic neuron health. Analysis of mutations in the *TNK2* gene highlight the clinical significance of this interface, whereby specific PD-patient associated variants cause increased TNK2 protein activity that results in the depletion of synaptic dopamine, sustained transport of small regulatory RNA molecules, and neurodegeneration.

Author contributions: J.B.N., H-A.P., K.A.C., and G.A.C. designed research; J.B.N., S.N.R., N.A.M., K.P., L.M.S., M.S., H-A.P., and K.A.C. performed research; J.B.N. contributed new reagents/analytic tools; J.B.N., S.N.R., H-A.P., K.A.C., and G.A.C. analyzed data; G.A.C. supervised the research project; and J.B.N., K.A.C., and G.A.C. wrote the paper.

The authors declare no competing interest.

This article is a PNAS Direct Submission.

[1]To whom correspondence may be addressed. Email: gcaldwel@ua.edu.

This article contains supporting information online at https://www.pnas.org/lookup/suppl/doi:10.1073/pnas.2210712120/-/DCSupplemental.

Published February 6, 2023.

in rat primary neuron cultures, as well as in patient-derived neurons from induced pluripotent stem cells (8, 9).

NEDD4 functions to modulate synaptic plasticity in a variety of ways (10), including through the cytoskeletal control of myelin compaction in oligodendrocytes (11), the ubiquitination of AMPARs response to amyloid-beta-peptide induced synaptic dysfunction (12), and in chronic stress response through ubiquitin-targeted degradation of the AMPAR subunit glutamate receptor 1, GluR1 (13). Moreover, NEDD4 appears to be both a target and effector of epigenetic regulation in the chronic stress response, where glutamatergic signaling, DNA methylation, histone modifications, and microRNAs (miRNAs) are all suspected determinants of resilience (14). Significantly, *NEDD4* was just recently found to be one of only five genes clinically associated with increased risk of epigenetic modulation in PD (15).

In the aforementioned WES study, four single nucleotide polymorphisms (SNPs) in *TNK2* were identified in PD patients (1). Based on the locations of these SNPs, we hypothesized that PD-associated TNK2 cannot be inactivated or evades being targeted for degradation by NEDD4 ubiquitination, thereby resulting in an improper regulation of DAT that ultimately leads to increased dopamine reuptake and disruption of dopaminergic signaling. An aberrant influx of dopamine not only weakens the synaptic dopaminergic signal but can also be toxic to presynaptic neurons due to dopamine-induced apoptosis (16). We previously demonstrated a selective vulnerability to dopamine-associated neurotoxicity in vivo, using both transgenic worm and mouse alpha-synuclein models of PD, where excess presynaptic dopamine biosynthesis correlated with increased neurodegeneration (17).

The *C. elegans* genome contains a single ortholog to human *TNK2* that is encoded by the *sid-3* (systemic RNAi defective-3) gene. The SID-3 protein is involved in modulating epigenetic signaling through regulating the cellular entry of double-stranded RNA molecules (dsRNAs), such as miRNAs (18). In worms and mice, respectively, SID-3 and TNK2 have been shown to be required for certain viral-RNA infections as demonstrated by genetic knockout studies (19, 20). The cells of *C. elegans* import dsRNA through the transmembrane transporter SID-1 (21), which is regulated by clathrin-dependent endocytosis (22). Whereas the understanding of organismal dsRNA transport in *C. elegans* is comparatively mature to that of more anatomically complex metazoans, the human genome encodes two gene products, SIDT1 and SIDT2, that have been purported to maintain a conserved role in the transport of extracellular dsRNA (23, 24, 25). Significantly, human SIDT2 was recently shown to be elevated in PD patient brains in conjunction with increased alpha-synuclein levels, and also colocalized to Lewy bodies (26). Thus, the functional duality represented by TNK2/SID-3 axis in the coordination of both dopamine and dsRNA import into the dopaminergic neurons of *C. elegans* warrants further mechanistic investigation.

We previously established *C. elegans* as a genetic animal model with which to investigate and reveal numerous conserved genes and cellular pathways underlying progressive dopaminergic neurodegeneration, often predating their association with PD in humans (9, 27–37). A distinct advantage of this model is the capacity to rapidly quantify dopaminergic neurodegeneration with precision, at the single-neuron level, and with rigor across large isogenic populations of animals per experiment (38, 39). As with mammalian PD toxin models, the uptake of dopamine through DAT-1, the *C. elegans* homolog of human DAT, can be measured indirectly through exposure to the selective neurotoxin, 6-hydroxydopamine (6-OHDA) (40). Similarly, the transport of dsRNAs by *C. elegans* SID-1, which is also localized on the plasma membrane (18), can be functionally quantified by fluorescence in response to RNAi knockdown of Green Fluorescent Protein (GFP). Through the application of these discrete bioassays, we describe a convergence of cellular mechanisms that impact dopaminergic neuron survival. Furthermore, we demonstrate that specific PD patient-associated SNPs in *TNK2* exert an analogous impact on dopaminergic neurodegeneration when introduced into the nematode counterpart, *sid-3*, by CRISPR gene editing. The research presented here illustrate a functional nexus whereby genetic mutations that influence dopamine levels in neurons intersect with the regulation of dsRNAs, key organismal modulators of epigenetic response, to modulate resilience or susceptibility to neurodegeneration.

Results

SID-3 Modulates 6-OHDA Neurotoxicity in *C. elegans*. Mammalian TNK2 has a regulatory function that serves to control dopamine synaptic and presynaptic dopamine levels by actively preventing clathrin-dependent endocytosis of the DAT (4). To determine if the *C. elegans* TNK2 ortholog, SID-3, similarly prohibits the endocytosis of the conserved worm DAT homolog, DAT-1, we treated *sid-3(ok973)* loss-of-function mutants (a 1,330 bp deletion allele) with 6-OHDA. Prior to 6-OHDA treatment, *sid-3(ok973)* worms were crossed into the wild-type (N2) background containing a chromosomally integrated transgene that enables GFP expression exclusively in dopamine neurons via the *dat-1* promoter [BY250; $P_{dat\text{-}1}$::GFP (*vtIs7*)] for visualization of neurodegeneration. Both *sid-3(ok973)* mutants and *sid-3* wildtype (GFP only) worms were assessed for degenerative changes in all six anterior DA neurons (39). If SID-3 and TNK2 share conserved roles in regulation of dopamine uptake through DAT/DAT-1, there should be a reduction in the uptake of 6-OHDA in *sid-3(ok973)* mutants, resulting in decreased neurodegeneration. Indeed, when compared with GFP-only control animals, the *sid-3(ok973)* mutants displayed robust protection from 6-OHDA, even at the highest concentration (50 mM), indicating an attenuation of dopamine uptake in the *sid-3(ok973)* mutant background, and evidence of functional homology between the human and worm proteins in the modulation of DAT-1 by endocytosis (Fig. 1 *A* and *C–F*). Invariably, we observe between 95 and 100% normal neurons in GFP-only expressing worms that are not treated with 6-OHDA, consistent with prior reports in the development of the 6-OHDA model (40). In Fig. 1*A*, worm population data are presented whereby if at least one neuron has degenerated, the animal is considered nonnormal. These data can also be represented as the severity of damage within the population of neurons (*SI Appendix*, Fig. S1*A*). The distribution of degenerating neurons parallels the trends and significance observed in the worm population data at all three concentrations (Fig. 1*A* vs. *SI Appendix*, Fig. S1*A*).

To support our findings implicating SID-3 in the regulation of DAT-1 endocytosis, we treated wild-type (GFP-only) animals with an established and selective TNK2 inhibitor, AIM-100 (41), that has been shown to inhibit the Tyr284-phosphorylation of TNK2 (42) and prevent the block it maintains on the endocytosis of mammalian DAT (4). Animals were treated daily with AIM-100 for 1-h, while control groups received only treatments with the solvent (1% ethanol). Like the *sid-3(ok973)* mutants, GFP-only animals treated with AIM-100 display significant protection from the neurotoxicity of 6-OHDA when compared with solvent controls (Fig. 1 *B* and *G*). Additionally, we treated *sid-3(ok973)* deletion mutants with AIM-100 to determine if the increase in neuroprotection

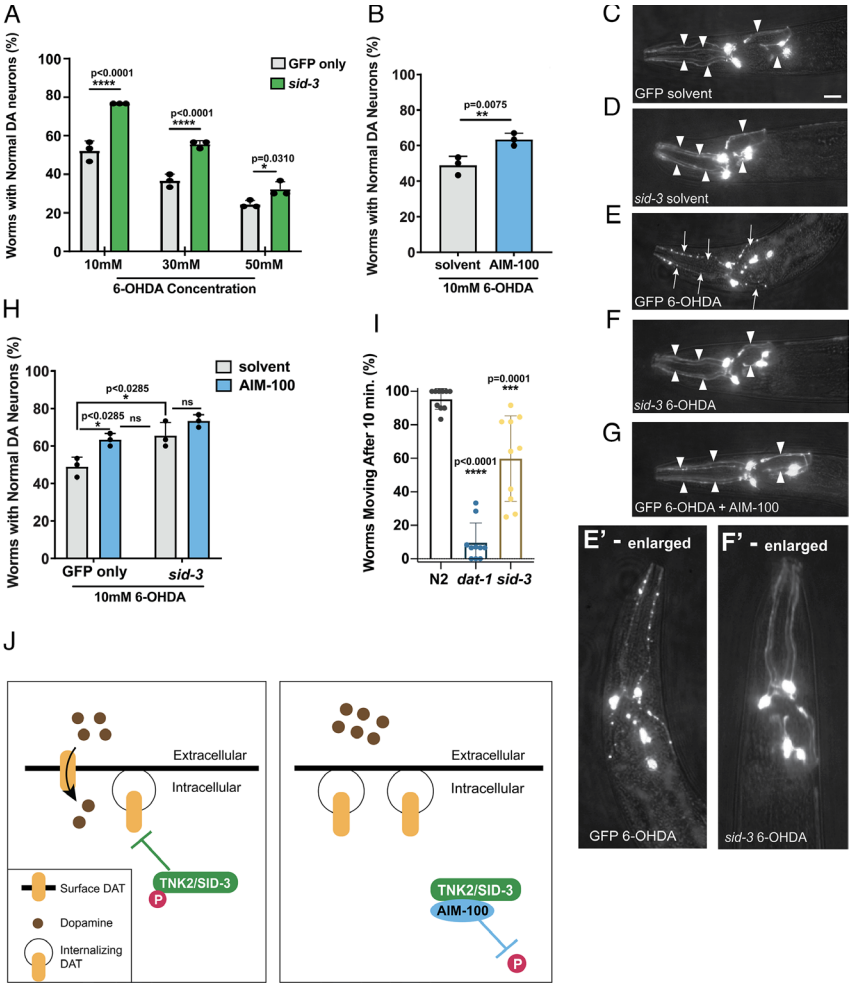

Fig. 1. Loss or inhibition of SID-3 function protects *C. elegans* dopaminergic neurons from 6-OHDA toxicity. (*A*) Both wild-type (strain N2) *C. elegans* (gray bars) and *sid-3(ok973)* loss-of-function mutants with dopaminergic GFP expression (green bars) were exposed to 6-OHDA. Bars represent mean values of N = 3. Error bars indicate SD; n = 30 worms in triplicate; two-way ANOVA with Sidak's multiple comparisons. (*B*) Wild-type control (N2) animals with only GFP expressed in dopaminergic neurons were treated with either 1% ethanol solvent (gray bar) or 100 µM AIM-100 (blue bar) and then subsequently assayed for neurodegeneration following treatment with 10 mM 6-OHDA. Bars represent mean values of N = 3. Error bars indicate SD with n = 30 worms in triplicate; Student's one-tailed *t* test. (*C–G*) Neuron images labeled to reflect specified conditions; arrowheads and arrows indicate intact or degenerated dopaminergic neurons, respectively. (Scale bar, 20 µm.) Images *E* and *F* are also enlarged, to enhance neuron visibility. (*H*) GFP-only control and *sid-3(ok973)* mutant animals treated with either 1% ethanol solvent (gray bars) or 100 µM AIM-100 (blue bars) and then assayed for neurodegeneration following exposure to 10 mM 6-OHDA. Bars represent mean values of N = 3. Error bars indicate SD with n = 30 worms in triplicate; two-way ANOVA with Tukey's post hoc multiple comparisons test. (*I*) Wild-type (N2) worms, and *dat-1(ok157)* or *sid-3(ok973)* deletion mutants were assayed for dopamine-specific behavioral change by swimming-induced paralysis (SWIP). Bars represent mean values of N = 10. Error bars indicate SD, with 10 to 15 animals scored per replicate; one-way ANOVA with Dunnett's post hoc multiple comparisons test. (*J*) Schematic model of TNK2/SID-3 regulation of DAT endocytosis. *Left* panel, baseline/wild-type conditions with activated TNK2/SID-3 blocking transporter endocytosis, thereby enabling 6-OHDA/dopamine uptake and neurodegeneration; *Right* panel, AIM-100 inhibition of TNK2/SID-3 phosphorylation results in diminished endocytic activity and protection from 6-OHDA neurotoxicity. TNK2/SID-3 (green); phosphate (pink); DAT (yellow); 6-OHDA/dopamine (brown); AIM-100 (blue).

observed in wild-type animals would be indicative of the drug possibly working through a target distinct from SID-3. AIM-100 did not enhance the neuroprotection of *sid-3(ok973)* mutants when compared with the solvent-only–treated *sid-3(ok973)* mutants (Fig. 1*H* and *SI Appendix*, Fig. S1*B*). Moreover, solvent-only–treated *sid-3(ok973)* mutants were not significantly different from AIM-100–treated (GFP-only) animals (Fig. 1*H* and *SI Appendix*, Fig. S1*B*). Considering the equivalence in neuroprotection observed with AIM-100–treated wildtype animals and untreated *sid-3(ok973)* mutants, and that this protection is abolished in a *sid-3 (ok973)* mutant background, it is reasonable to conclude that SID-3 is the target of AIM-100 and that this drug provides neuroprotection by attenuating 6-OHDA uptake into the dopaminergic neurons of *C. elegans*.

To further demonstrate the impact of SID-3 on dopamine uptake in *C. elegans*, we conducted a behavioral analysis where we monitored *sid-3(ok973)* mutants in swimming-induced paralysis (SWIP) assays (43). SWIP assays are used as an indirect measure of proper synaptic dopamine clearance. Animals that display significantly aberrant dopamine clearance undergo paralysis after 10 minutes of thrashing in water, while animals with intact dopamine clearance can thrash continuously (43). Our results, as depicted in Fig. 1*I*, demonstrate that *sid-3(ok973)* animals exhibited significantly more paralysis than did wild-type (N2) controls after 10 min of thrashing. However, this was not as significant as *dat-1 (ok157)* loss-of-function mutants (Fig. 1*I*). It is not surprising that *sid-3(ok973)* mutants do not have as pronounced of an effect as the *dat-1* deletion mutants since a limited pool of DAT would remain at the presynaptic plasma membrane, albeit undergoing an increase in basal internalization (44). Ideally, measurements of DAT-1 levels at the presynaptic membrane would be evaluated, but the small size and limited number of dopaminergic neurons in *C. elegans* preclude such quantitative analyses.

Collectively, these results, using both genetic and pharmacological modifiers, suggest that SID-3 retains a conserved function of mammalian TNK2 in preventing the endocytic internalization of DAT (Fig. 1*J*). This model predicts that either deletion [*sid-3(ok973)*] or inhibition [by AIM-100] of SID-3/TNK2 activity would be neuroprotective, with a net increase of synaptic dopamine resulting in enhanced dopaminergic neurotransmission. These results suggested to us that the dominantly inherited SNPs in the *TNK2* gene of PD patients were potentially representative of *increased* TNK2 stability and/or activity.

NAB2-Induced Neuroprotection Requires the *C. elegans* NEDD4 Homolog, WWP-1. Since a constitutive blockade of DAT endocytosis by TNK2 would rapidly deplete the levels of synaptic dopamine, it is critical that the dopaminergic system be both dynamic and responsive to a variety of conditions. NEDD4 is a E3 ubiquitin ligase known to ubiquitinate TNK2 for degradation (6, 45). To determine if increasing the activity of the NEDD4 homolog in *C. elegans*, WW domain-containing protein 1 (WWP-1), would lead to neuroprotection from 6-OHDA, we treated wild-type (GFP-only) animals with a previously defined and selective NEDD4 activator, NAB2 (9). If NEDD4 has a regulatory effect on DAT internalization by targeting TNK2/SID-3 for degradation, then an increase in NEDD4/WWP-1 activity would result in a reduction

in 6-OHDA import, and neuroprotection. Indeed, when compared with solvent-treated controls, NAB2-treated animals were protected from 6-OHDA-induced neurodegeneration (Fig. 2*A*), in accordance with prior work where we demonstrated that alpha-synuclein-induced toxicity was attenuated by NAB2 treatment in transgenic *C. elegans*, complementing supporting results in both yeast and rat primary neurons (9). It should be noted that, because the *C. elegans* genome lacks an endogenous alpha-synuclein gene, our findings acquired in the complete absence of alpha-synuclein are mechanistically significant, since alpha-synuclein was reported to be a direct target of NEDD4-dependent ubiquitination and degraded through endolysosomal clearance (46). Taken together, the regulatory node centered at NEDD4/TNK-2 functionality promotes neuroprotection through multiple means.

Although *C. elegans* WWP-1 shares the highest overall amino acid sequence homology and conserved domain structure with human NEDD4, and *wwp-1* is highly expressed in the nervous system, the worm genome contains multiple E3 ligases that share varying degrees of homology with NEDD4. Therefore, to confirm that the observed responses to NAB2 were a consequence of its action on WWP-1, we crossed animals with a WWP-1 null mutant, *wwp-1(gk372)* (47, 48), into GFP-only animals and assayed these with 6-OHDA and NAB2 treatments. Animals in the *wwp-1(gk372)* mutant background showed a complete abolishment of NAB2-induced neuroprotection from 6-OHDA, while control animals retained NAB2-neuroprotection (Fig. 2*B*), thereby demonstrating that NAB2 acts through the NEDD4 homolog, WWP-1, in *C. elegans*. We also note that the *wwp-1(gk372)* mutation did not enhance neurodegeneration independently (Fig. 2*B*). We also wanted to examine if NAB2-neuroprotection from 6-OHDA operates through the targeting of SID-3 by WWP-1 for degradation, consequentially enabling DAT-1 internalization. As shown in Fig. 2*C*, treatment of *sid-3(ok973)* mutants either with NAB2 or its solvent control did not affect the dopaminergic neuroprotection that was displayed in the absence of SID-3 function (Fig. 2*C*). Furthermore, NAB2 treatment of wild-type (GFP-only) worms offered a similar level of protection from 6-OHDA neurotoxicity as was observed with *sid-3(ok973)* mutant controls (Fig. 2*C*). Thus, in terms of neuroprotection, the activation of NEDD4/WWP-1 by NAB2 phenocopies the complete depletion of TNK2/SID-3 in *C. elegans*.

Activation of NEDD4 in Rat Primary Neurons Leads to a Reduction in Endogenous TNK2 and Neuroprotection from 6-OHDA. To determine whether the proposed mechanism of dopaminergic regulation we have elucidated in *C. elegans* translates to mammals, we examined rat cortical primary neurons for evidence of a change in TNK2 levels following activation of NEDD4 by NAB2. We previously reported that rat primary neurons exhibited neuroprotection in response to NAB2 treatment (9). Indeed, this effect further translated to human neurons derived from iPSCs of PD patients (8). It remains to be discerned whether the neuroprotective effects observed are a potential consequence of a decrease in TNK2 levels. We demonstrated that enhancement of NEDD4 activity by NAB2 treatment lowers endogenous neuronal TNK2 protein levels (Fig. 2*D*). Similar to the worm experiments

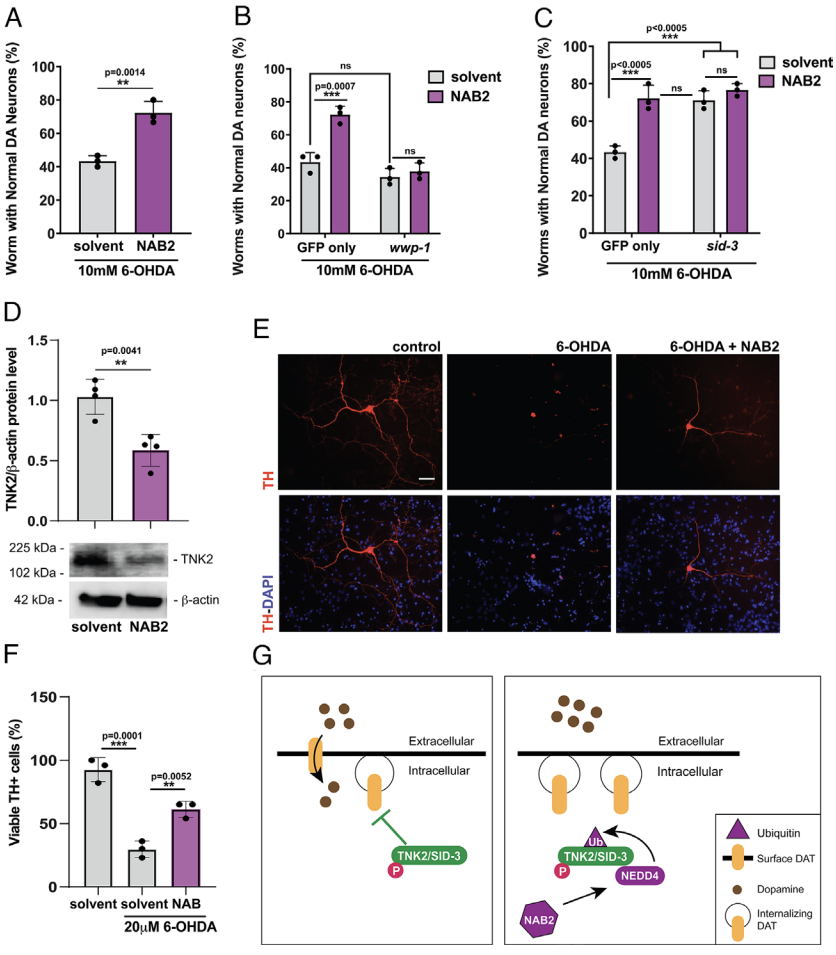

Fig. 2. NAB2 treatment results in neuroprotection and decreased TNK2 levels in rat primary neuron cultures and exhibits NEDD4/WWP-1-dependent neuroprotection from 6-OHDA exposures in *C. elegans*. (*A–C*) Specified worm strains treated with 100 μM NAB2 (purple bars) or 1% ethanol solvent (gray bars) received a 1-h treatment each day before exposure to 10 mM 6-OHDA. (*A*) Wild-type GFP-only control animals, where bars represent mean values of N = 3. Error bars indicate SD with n = 30 worms in triplicate; Student's one-tailed *t* test. (*B*) GFP-only and *wwp-1(gk372)* loss-of-function animals, where bars represent mean values of N = 3. Error bars indicate SD with n = 30 worms in triplicate; two-way ANOVA with Tukey's multiple comparisons. (*C*) GFP-only and *sid-3(ok973)* animals, where bars represent mean values of N = 3. Error bars indicate SD with n = 30 worms in triplicate; two-way ANOVA with Tukey's multiple comparisons. (*D*) Rat cortical neurons were treated with 2 μM NAB2 or solvent control [dimethyl sulfoxide (DMSO)], and western blotting was used to detect TNK2. A representative blot is shown with the accompanying graph representing the mean of four experiments, indicates a significant decrease in TNK2 protein levels in response to NAB2. Error bars indicate SEM; Student's two-tailed *t* test. (*E* and *F*) Rat dopaminergic neurons were treated with NAB2 or DMSO (the solvent for NAB2) t and 20 mM 6-OHDA. Tyrosine hydroxylase-positive (TH+) neurons were assessed by immunocytochemistry. NAB2 treatment prevents the dopamine neuron degeneration induced by 6-OHDA. (*E*) Representative neurons; (Scale bar, 50 μm.) Red: TH+ cells; Blue: DAPI+ cells. (*F*) Quantitative analysis of viable TH+ dopaminergic cells where bars represent mean values of N = 3, error bars indicate SEM with 20 to 30 micrographs counted per experiment: one-way ANOVA with Tukey's multiple comparisons. (*G*) Schematic diagrams depicting regulation of DAT endocytosis and dopamine/6-OHDA uptake by TNK2/SID-3 (*Left*); ubiquitination of TNK2/SID-3 in response to NAB2 activation of NEDD4/WWP-1 (*Right*) reduces TNK2/SID-3 levels, leading to DAT endocytosis, higher levels of dopamine in the synapse, and enhanced neuroprotection from 6-OHDA toxicity. TNK2/SID-3 (green); phosphate (pink); DAT (yellow); dopamine/6-OHDA (brown); NEDD4 (purple); NAB2 (purple hexagon); Ubiquitin (purple triangle).

described in 2A, we wanted to determine if increasing the activity of NEDD4 in rat primary dopaminergic neurons would lead to neuroprotection from 6-OHDA. Cultured neurons were treated to NAB2, with or without 6-OHDA for 24 h (Fig. 2 *E* and *F*). The control group was treated with the solvent only. Compared with solvent-treated controls, there were more Tyrosine hydroxylase-positive viable neurons in the NAB2-treated group (Fig. 2 *E* and *F*), consistent with the neuroprotection observed in *C. elegans* (Fig. 2*A*). The combined outcomes of these studies can be summarized by a model (Fig. 2*G*) that portrays both the targeting of TNK2 for degradation via the ubiquitin-proteasome system and altered endocytic regulation as potential cellular mechanisms amenable to fine-tuning of dopamine levels to sustain optimal dopaminergic neurotransmission and health.

SID-3 Facilitates dsRNA-Mediated Gene Silencing in *C. elegans* Dopaminergic Neurons. SID-1-dependent transport of dsRNA in *C. elegans* is modulated through the internalization of this plasma membrane protein by clathrin-dependent endocytosis (22). Previous studies reported that SID-3 plays a functional role in support of the systemic spread of dsRNA between the somatic cells of *C. elegans*, with a concomitant impact on the efficacy of RNAi (18). Just as TNK2 regulates the clathrin-dependent endocytosis of DAT to modulate dopamine reuptake, it has been hypothesized that SID-3 functions as an endocytic modulator of dsRNA uptake by preventing the clathrin-dependent endocytosis of SID-1 (18). To determine whether SID-3 regulates dopaminergic RNAi, we fed animals RNAi-inducing bacteria engineered to produce exogenous dsRNA-targeting GFP that was expressed exclusively in the dopaminergic neurons. Due to an inherently RNAi-resistant nature of neurons in *C. elegans* (49), GFP-only and *sid-3(ok973)* animals were crossed into an RNAi-hypersensitive background, *eri-1(mg366)*, which does not impact the transport of dsRNAs but rather has changes in exonuclease and nucleic-acid-binding activity that facilitate RNAi efficacy (50). Subsequent RNAi knockdown in wild-type animals led to silencing of GFP fluorescence, when compared with empty vector (EV) RNAi control (Fig. 3 *A*, *C*, and *D*). In contrast, *sid-3(ok973)* mutants displayed significantly less dopaminergic neuron silencing compared with wild-type animals (Fig. 3 *A* and *E*). As has been previously reported for *sid-3* mutants in other cell types a loss of SID-3 activity diminished, but did not completely abolish, RNAi silencing (18), This can be visualized by examining the severity of damage within populations of neurons (*SI Appendix*, Fig. S2*A*). This expected result is indicative of increased endocytosis of SID-1 at the plasma membrane, where a modicum of this dsRNA transporter likely remains present (Fig. 3*G*).

We further demonstrated the necessity of active SID-3 for dsRNA-induced silencing in the dopaminergic neurons by treating animals with AIM-100. Wild-type worms treated with AIM-100 exhibited a decrease in dopaminergic neuron fluorescence in response to RNAi knockdown of GFP when compared with solvent-only controls (Fig. 3 *B* and *F* and *SI Appendix*, Fig. S2*B*). This result was consistent with our prior data demonstrating that both AIM-100 treatment of wild-type animals and *sid-3(ok973)* mutants similarly displayed neuroprotection from 6-OHDA (Fig. 1 *A* and *B*). In this case, however, lifting the block on dsRNA uptake as a response to AIM-100 inhibition of SID-3 results in an increased capacity to respond to dsRNA that is readily observed through the efficacy of gene silencing (Fig. 2*G*). In contrast to AIM-100 (Fig. 3 *B* and *F*), a distinction with NAB2 treatment was observed, as this NEDD4 activator did not significantly alter the efficacy of GFP RNAi silencing in dopaminergic neurons (Fig. 3*I* and *SI Appendix*, Fig. S2*C*).

In considering the robust neuroprotection observed with *sid-3(ok973)* mutants, we reasoned that the effect could be partially attributed to the diminished import of silencing dsRNAs. To test this hypothesis, we assayed *sid-1(pk3321)* loss-of-function mutants with 6-OHDA and compared the results with *sid-3(ok973)* or *sid-1(pk3321)*; *sid-3(ok973)* double mutants, as well as wild-type (GFP-only) control animals (Fig. 3*H*). Although depletion of the SID-1 dsRNA transporter in *sid-1(pk3321)* mutants was neuroprotective against 6-OHDA, compared with GFP only control animals, it was not as nearly protective as observed in the *sid-3(ok973)* deletion mutants. Likewise, *sid-1(pk3321)*; *sid-3(ok973)* double mutants also displayed significantly increased levels of neuroprotection, similar to *sid-3 (ok973)* alone (Fig. 3*H*). Superficially, these data could be suggestive of an epistatic relationship between the *sid-1* and *sid-3* alleles. Yet, in the specific case of the dopaminergic system, the enhanced neuroprotection exhibited in *sid-3(ok973)*, along with evidence of intersecting regulation of dopamine and dsRNA uptake by SID-3, suggests that a more complex regulatory dynamic is at work in response to the acute neurodegenerative challenge presented by 6-OHDA treatment.

Consequences of PD-Patient-Associated SNPs on TNK2/SID-3 Function In Vivo. *TNK2* encodes a nonreceptor tyrosine kinase with a unique domain structure that is conserved in *C. elegans* SID-3 (Fig. 4*A*). Mutations in *TNK2* have been identified in several types of cancers (51). Among protein regions that are mutated are the protein kinase domain (PKD), a proline-rich NEDD4-interacting region (P), and ubiquitin-associated domain (UBA). Previous research focused on infantile-onset epilepsy showed that a similar mutation of *TNK2* in the proline-rich region blocked its interaction with NEDD4, eventually leading to infant mortality (52). Of particular interest to our study, SNPs within *TNK2* discovered through WES of DNA from patients with familial PD include variants in some of these predicted functional domains (1) (Fig. 4*A*). The only two nonreceptor tyrosine kinases in humans that have a UBA domain are TNK2 and a less studied paralog, TNK1(53). However, the structure of TNK1 diverges from that of TNK2, as the former kinase lacks all other predicted functional domains found in TNK2 (Fig. 2*A*). While both *TNK1* and *TNK2* are expressed ubiquitously and have been investigated for their function in cancers (51, 53), only *TNK2* is most highly expressed in the brain and is altered in patients with PD (1). Although *TNK1* transcription is at its lowest levels in neurons, it has been recently identified as containing variants of unknown significance in patient samples from a study of early-onset dementia (54).

We sought to determine if two of the PD patient-associated SNPs located in conserved sites of posttranslational regulation of TNK2/SID-3 activity (PKD) or stability (UBA domain) confer an increased susceptibility to neuronal dysfunction and/or survival. To examine these SNPs in vivo, we used CRISPR technology to edit the chromosomal *C. elegans sid-3* gene and thereby generate two separate strains encoding SNPs in either the conserved PKD or UBA domains of the endogenous gene product that reflected the variants found in PD patients (1) (Fig. 4*A*). We first tested whether the modified nematodes containing these specific SNPs exhibited an enhanced susceptibility to 6-OHDA-induced neurodegeneration. However, no increase in dopaminergic neurodegeneration was observed in animals using the standard assay conditions for exposure, 10 mM 6-OHDA (Fig. 4*B*). We reasoned that the acute neurotoxicity of 10 mM 6-OHDA could mask the impact of either genetic background. Therefore, we decided to halve the dosage to provide for a more sensitive test. Exposure to 5 mM 6-OHDA revealed that the SNP-containing worms showed significantly more neurodegeneration, and that these animals were

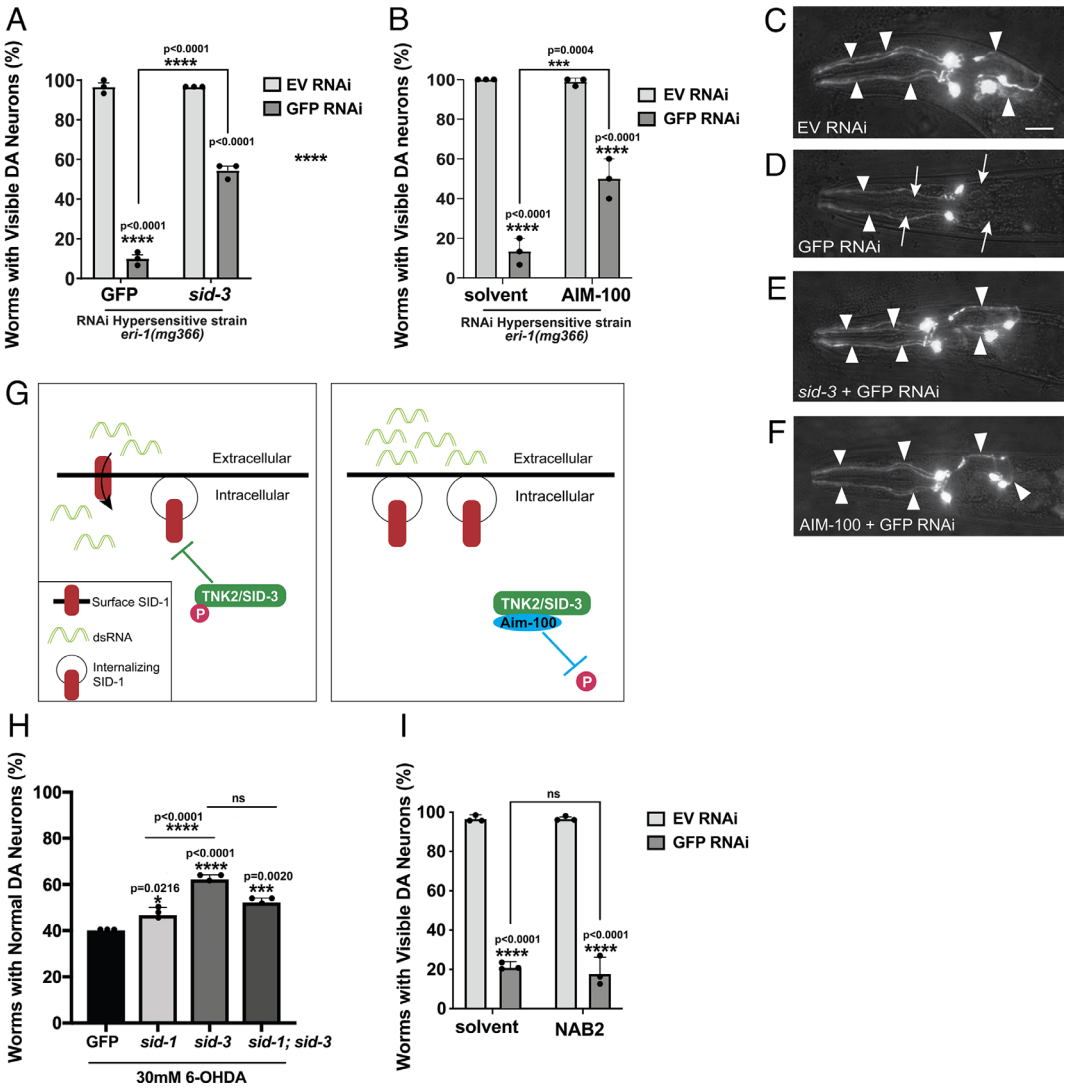

Fig. 3. Loss or inhibition of SID-3 decreases dopaminergic RNAi efficacy in *C. elegans*. (*A*) Animals expressing GFP in the dopaminergic neurons of both control (wild-type; GFP-only) and *sid-3(ok973)* mutant animals in an RNAi-hypersensitive background [*eri-1(mg366)*] fed bacteria harboring dsRNA targeting GFP (dark gray bars) or EV (light gray bars). Bars represent mean values of N = 3. Error bars indicate SD with n = 30 worms in triplicate; two-way ANOVA with Tukey's post hoc multiple comparisons test. (*B*) GFP-only animals in a RNAi-hypersensitive background raised on RNAi plates with or without 100 µM AIM-100 added to the agar. Bars represent mean values of N = 3. Error bars indicate SD with n = 30 worms in triplicate; two-way ANOVA with Tukey's post hoc multiple comparisons test. (*C–F*) Representative dopaminergic neuron images of worms from experiments in panels *A* and *B* where neurons are either still visible (arrowheads) or GFP is silenced (arrows). (Scale bar, 20 µm.) (*G*) Schematic diagram of TNK2/SID-3 regulation of dsRNA import. *Left* panel depicts activated TNK2/SID-3 preventing the endocytosis of SID-1, thereby facilitating dsRNA transport; *Right* panel, inhibition of TNK2/SID-3 activity by AIM-100 releases the block on endocytosis, causing resistance to dsRNA transport. TNK2/SID-3 (green); phosphate (pink); SID-1 (red); dsRNA (light green); AIM-100 (blue). (*H*) Direct comparison of wild-type control (GFP-only), *sid-1(pk3321), sid-3(ok973),* or *sid-1(pk3321);sid-3(ok973)* double mutants when exposed to 30 mM 6-OHDA. Distinctions potentially reflect the relative contributions to neuroprotection from dsRNA uptake and/or dopamine (6-OHDA) transport. Bars represent mean values of N = 3. Error bars indicate SD with n = 30 worms in triplicate; one-way ANOVA with Tukey's multiple comparisons. (*I*) GFP-only animals in a RNAi-hypersensitive background raised on RNAi plates with or without NAB2 (100 µM) added to the agar do not exhibit a significant change in RNAi efficacy. Bars represent mean values of N = 3. Error bars indicate SD with n = 30 worms in triplicate; two-way ANOVA with Tukey's post hoc multiple comparisons test.

more sensitive to the lower dosage of neurotoxin than their WT counterparts (Fig. 4*C*). These results provide mechanistic evidence for these specific PD-patient SNPs in TNK2/SID-3 functionally altering dopamine uptake, as revealed via its neurotoxic proxy molecule, 6-OHDA.

We next wanted to evaluate these same PD-patient SNPs for their impact on dsRNA import to induce RNAi silencing in *C. elegans*. Therefore, both CRISPR-edited strains were crossed into the hypersensitive *eri-1(mg366)* background and fed RNAi bacteria selectively targeting GFP. Both the PKD and UBA domain-associated SNPs led to very pronounced GFP silencing in the dopaminergic neurons (Fig. 4*D*). This was striking when compared with the resistance to RNAi observed in *sid-3(ok973)* loss-of-function mutant animals within the same hypersensitive background. In fact, the level of RNAi knockdown observed in either of the CRISPR-edited strains was largely equivalent to the activity observed in nonmutant controls.

To further investigate the functional consequences of these polymorphisms, we examined whether the NAB2-induced neuroprotection previously observed remained intact in animals encoding SID-3 with the UBA domain-associated SNP. Interestingly, NAB2 was no longer neuroprotective against 6-OHDA in these SNP-containing animals (Fig. 4*E*). This indicates that the interaction between SID-3 and WWP-1 was abolished and is necessary for proper DAT-1 regulation (Fig. 4*G*). These data are consistent with studies done in mammalian cell cultures on similar, but not PD-associated, *TNK2* variants harboring SNPs shown to disrupt NEDD4-TNK2 interactions (52). Therefore, failure of

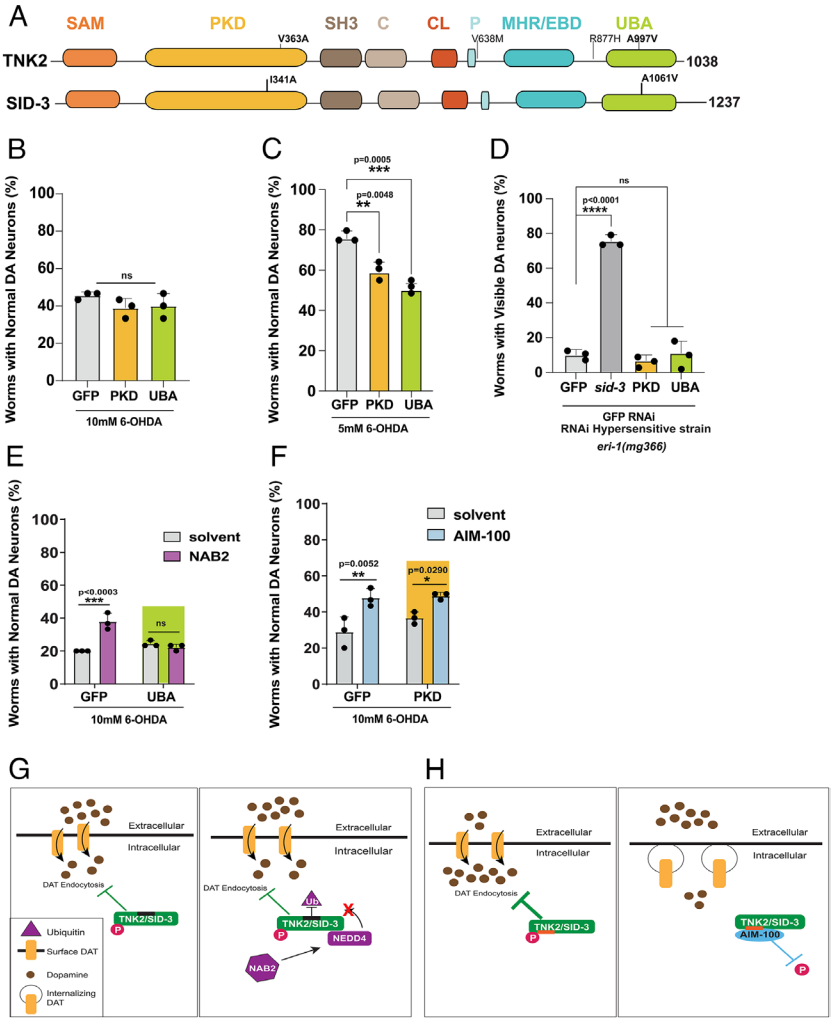

Fig. 4. Functional effects of PD-related SNPs in *TNK2* at analogous positions in *sid-3* of CRISPR-edited *C. elegans*. (*A*) Protein domains of human TNK2 share homology with SID-3. SAM = sterile alpha motif; PKD = tyrosine protein kinase domain; SH3 = Src homology domain; C = CDC42-binding domain; CL = clathrin-interaction domain; P = proline rich motif containing the NEDD4 binding site; MHR/EBD = MIG6 homology region (also known as an epidermal growth factor receptor binding domain or EBD); UBA = ubiquitin-associated domain. Amino acid changes resulting from the PD-related SNPs in human *TNK2* are indicated in black; the CRISPR-edited sites in the corresponding SID-3 protein of *C. elegans* are indicated, with the human SNPs bolded. (*B*) Wild-type SID-3 control (GFP only) or CRISPR-edited animals containing analogous changes to the PKD in SID-3(I341A) or the UBA-domain SID-3(A1016V) exposed to either 10mM 6-OHDA or (*C*) 5mM 6-OHDA. (*D*) RNAi-hypersensitive worms in either the GFP-only (WT SID-3), *sid-3(ok973)* deletion mutant, or CRISPR-edited backgrounds (with PKD or UBA SNPs) following RNAi feeding with bacteria targeting GFP for two generations. (*B–D*) Bars represent mean values of N = 3. Error bars indicate SD with n = 30 worms in triplicate; one-way ANOVA with Dunnett's post hoc multiple comparisons test. (*E*) Animals with the UBA-domain SNP treated with 100 μM NAB2 are not protected from 6-OHDA-induced neurodegeneration. Bars represent mean values of N = 3. Error bars indicate SD with n = 30 worms in triplicate; two-way ANOVA with Sidak's post hoc multiple comparisons test. (*F*) Animals with the PKD SNP treated with 100 μM AIM-100 are still protected from 6-OHDA. Bars represent mean values of N = 3. Error bars indicate SD with n = 30 worms in triplicate; two-way ANOVA with Sidak's post hoc multiple comparisons test. (*G*) SID-3 containing the PD-patient-derived SNP in the UBA domain at an analogous position that found in TNK2 is depicted as being targeted for ubiquitin-mediated degradation without (*Left*) and with (*Right*) NAB2-activated NEDD4 E3 ligase activity, which is blocked by the UBA-domain SNP (H) SID-3 engineered to contain the PD-patient-derived SNP found in the PKD of TNK2 is depicted as hyperactive in preventing DAT endocytosis, thereby resulting in depletion of synaptic dopamine (*Left*); this SNP does not impact the ability of SID-3 to be inactivated by AIM-100, and therefore retains the capacity for DAT internalization and neuroprotection (*Right*). TNK2/SID-3 (green with dark purple bar representing UBA-SNP); or (green with orange bar representing PKD-SNP); phosphate (pink); DAT (yellow); dopamine (brown); NEDD4 (purple); NAB2 (purple hexagon); Ubiquitin (purple triangle).

NEDD4-dependent degradation of TNK2 provides a mechanism to explain how patients harboring a dominant missense substitution in the *TNK2* UBA domain manifest with the symptoms of PD as a consequence of increased DAT-mediated reuptake of dopamine and a reduction in synaptic dopamine.

Treatment of *C. elegans* with the TNK2 inhibitor, AIM-100, leads to neuroprotection in a manner that phenocopies SID-3 loss-of-function [(*sid-3 (ok973)*] (Fig. 1 *A* and *B*). In contrast, when CRISPR-edited worms containing a SNP in the PKD of SID-3 were treated with AIM-100, neuroprotection persisted (Fig. 4*F*). Notably, a similar PKD variant in human TNK2 was found in prostate cancer that increased TNK2 activity (42). In the dopaminergic system, where we have demonstrated that depletion of this gene product is neuroprotective, a hyperactive TNK2/SID-3 would be predicted to exert detrimental consequences that could contribute to PD. Importantly, it was determined that AIM-100 still functioned to prevent the phosphorylation of TNK2 in the hyperactive variant (42), thereby correlating with our observation that AIM-100 retains its inhibitory/protective activity even when SID-3 contains an analogous SNP. Thus, in the absence of AIM-100, these same CRISPR-modified animals are no longer protected from neurodegeneration (Fig. 4 *F* and *H*). These results define the clinical impact of polymorphisms in *TNK2*, identified by WES of PD patients, as an outcome of a lost cellular capacity to either degrade or inactivate this pivotal enzyme.

Discussion

The symptomatic phenotypes of PD are largely a result of the death of dopaminergic neurons located in the *substantia nigra*. The clinical emergence of symptoms, such as resting tremor and rigidity, arise only once 50 to 80% of the dopaminergic neurons are lost yet the age of onset can vary dramatically among individuals (55). The search to uncover new genetic associations with PD is ongoing, and the significance of distinct cellular pathways that impact the dopaminergic system, and the intersection of them, will be critical to defining prognosis and closing the gap between diagnosis and treatment. A prerequisite to an eventual understanding of gene-by-environmental contributions in discerning disease risk is a mechanistic means through which their combined effects are manifested. A failure of such integrated processes may underlie differential susceptibility to disease, and as demonstrated here, the neurodegeneration observed in individuals with PD. Our findings collectively support a molecular model for dopaminergic neuroprotection that reflects how the neuromodulation of synaptic and intracellular dopamine levels directly converges with the organismal machinery required to transmit exogenous influences on gene expression conferred through noncoding small RNAs (Fig. 5).

As human genomic data flood the present research landscape with tantalizing associations and clues to disease mechanisms, the challenging task to functionally annotate these genomic

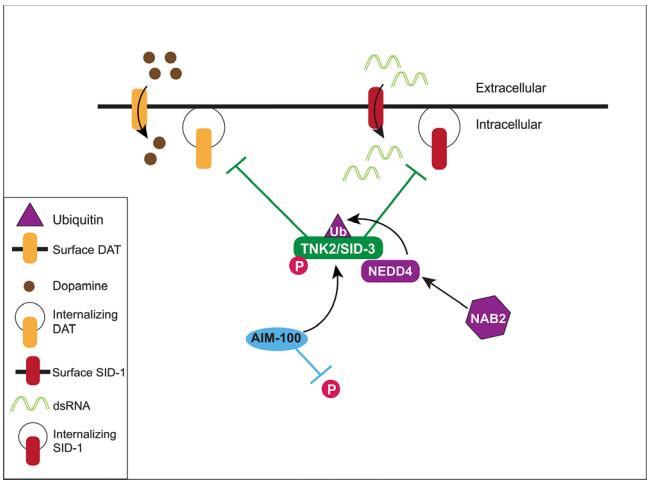

Fig. 5. Model depicting the integrated dopaminergic and epigenetic modulation of neuroprotection through TNK2/SID-3. The endocytosis of the DAT, is necessary for maintaining levels of synaptic and presynaptic dopamine in a healthy balance that ensures proper neurotransmission. As shown above, the nonreceptor tyrosine-kinase, TNK2, maintains a functional hold on the endocytosis of the DAT, in the regulation of dopamine levels. NEDD4, an evolutionarily conserved E3 ubiquitin ligase, interacts with TNK2, and targets it for degradation by the ubiquitin-proteasome system (UPS). We demonstrated that NEDD4 activation, which is induced by treatment with the small molecule, NAB2, attenuates dopaminergic neurodegeneration induced by the neurotoxic dopamine analog, 6-OHDA, in both in *C. elegans* and rat primary neuron cultures. In an analogous manner, the *C. elegans* TNK2 ortholog, SID-3, is known to be required for epigenetic gene silencing, as a result of its function in systemic RNAi through the regulation of the SID-1 dsRNA transporter protein. We hypothesized that inhibition or loss-of-function of TNK2/SID-3 results in the endocytosis of DAT and SID-1, limiting the amount of dopamine and dsRNA transported, respectively, into cells. Conversely, if TNK2/SID-3 is activated, endocytosis of these dual transporters is blocked and their activity at the presynaptic membrane surface results in constitutive removal of dopamine from the synapse (or uptake of 6-OHDA), as well as dysregulated and continuous dsRNA uptake. Our results show that either genomic deletion or chemical (AIM-100) inhibition of SID-3 abolished dsRNA-targeted silencing of gene expression in worm dopamine neurons—in addition to protecting both *C. elegans* and rat primary dopamine neurons from 6-OHDA neurotoxicity. We used *C. elegans* to functionally examine why this protective capacity is lost in PD patients that contain SNPs in *TNK2.* By engineering SID-3 in worms to mimic specific PD-patient SNPs found in *TNK2,* we have revealed that the mechanism of neurodegeneration in these patients is likely not due to a loss-of-function but is instead a consequence of sustained TNK2/SID-3 activity that affects both dopamine levels and dsRNA-mediated gene silencing. The functional convergence and integrated control of dopaminergic and epigenetic mechanisms depicted in this model has substantial implications for how neurodegeneration can be modulated in PD. TNK2/SID-3 (green); phosphate (pink); DAT (orange); dopamine/6-OHDA (brown); AIM-100 (blue); SID-1 (red); dsRNA (light green); NEDD4 (purple); NAB2 (purple hexagon); Ubiquitin (purple triangle).

variants has become increasingly significant. Research consortia have arisen to tackle the challenges of rare and undiagnosed diseases (56–59), joining the efforts of individual labs in parsing the data deluge with experimentation to accelerate therapeutic target and drug discovery for more common diseases as well (37, 60–63). These collective efforts have begun to bear fruit, and they are not limited to the direct relationship between genotype and phenotype alone. Experimental strategies inclusive of the complexities introduced by epigenetic regulation, layered on a background of disease-modifying factors, represent a next level of functional genomic analysis (64, 65). As the present study strives to impart, the directed application of invertebrate model systems serves as a means to advance functional annotation of human genomic variation, inform therapeutic discovery, and accelerate clinical understanding (66).

Fundamental organismal strategies acting as drivers of evolutionary change typically manifest as an increased capacity to adapt to fluctuating environments. This is epitomized by the epigenetic control of gene expression (67). Medical research has merely scratched the surface of what must urgently be understood to attain a clearer picture of how external (environmental) epigenetic influences on organismal health intersect with heritable or de novo genetic susceptibilities to manifest in disease states. A quantitative measure, termed stochastic epigenetic mutation (SEM), was devised to represent dysregulation at sites of genomic DNA methylation, an epigenetic hallmark that increases with chronological age (68). More recently, another metric, epigenetic mutation load (EML), has been applied by clinical researchers to the analysis of PD risk (15). EML represents the aggregate value of SEMs within the genome of an individual and is intended to reflect overall change or failure of epigenetic maintenance systems. Application of EML analysis to patient data on PD-associated loci revealed genes at greater risk of being affected by epigenetic modulation. In considering the translational significance of our findings, it is validating to note that *NEDD4* was among a short list of only five such genes identified as having the strongest correlation with epigenetic modulation in PD patients (15).

We therefore attempted to discern the mechanistic significance of TNK2/SID-3 activity in PD by addressing three key points: 1) We determined that SID-3 retains the conserved role of TNK2 in modulating reuptake of dopamine in *C. elegans*; 2) we found that SID-3 also regulates the capacity for dsRNA-induced gene silencing in the dopaminergic neurons and that this modulates neurodegeneration; and 3) we evaluated the functional consequences of PD patient-associated SNPs in TNK2 using SID-3 for their respective impact on neurodegeneration and dsRNA-mediated gene silencing in vivo. Our findings indicate that genomic variants of *TNK2* found in patients define a molecular etiology for PD in which neurodegeneration is a consequence of dysfunctional cellular dynamics at an intersection of dopaminergic and epigenetic signaling.

The core cellular machinery for dopamine biosynthesis, vesicular packaging, transport, and neurotransmission is highly conserved among metazoans, as is the tight regulation of its component proteins. Invertebrate species, most prominently *Drosophila melanogaster* and *C. elegans*, have provided numerous insights into mechanistic features of dopaminergic neurotransmission and neurodegeneration (66, 69–71). Although the genes for key enzymes and proteins (i.e., *DICER1*, *DROSHA1*, Argonauts) underlying a capacity for RNAi appear to have been evolutionarily maintained, a functional divergence among the precise miRNA sequences that trigger gene silencing is evident among species (72). Mechanistic differences in the intercellular transport and systemic distribution of small RNA modifiers of gene expression presumptively represent another logical point of divergence between anatomically distinct organisms. Despite extensive therapeutic interest and success in dsRNA delivery to mammalian cells, it is surprising that systemic mechanisms of small RNA distribution and import in humans remain elusive and largely uncharacterized since the pioneering discoveries of RNAi and miRNAs were made using *C. elegans* (73–75).

Two mammalian orthologs of *C. elegans* SID-1 encoded within human genome are SIDT1 and SIDT2 (76, 77). Contradictory reports on whether or not these proteins function as dsRNA transporters currently hinder a more definitive classification of their activities. Multiple studies support a role for SIDT1 in dsRNA and miRNA transport in human cells (23, 25, 78). Sidt1 (–/–) knockout mice have also been generated that lack an ability to absorb dietary miRNAs in the gut (79). Sidt2 is highly expressed in several tissues including the brain, intestine, liver, and kidneys of rats (80). Sidt2 (–/–)-deficient mice have been associated with

impaired glucose tolerance (81), but conversely exhibit reduced tumor burden in lung and gastrointestinal cancer models (25). On the contrary, other reports using HEK293, PANC-1 or *Drosophila* S2 cells, reported that both SIDT1 and SIDT2 lack dsRNA transport activity, and are instead required for the translocation of cholesterol (82, 83). Overexpression of either human SIDT1 or SIDT2, or SID-1 of *C. elegans,* in HEK293 cells revealed that radiolabeled dsRNA uptake displayed a dose-dependent response to cholesterol addition (84). Furthermore, innate immunity in *C. elegans,* which is a cholesterol auxotroph, requires the function of the CHUP-1 cholesterol transporter, a structural but not functional ortholog of SID-1, as well as human SIDT1 and SIDT2 (84, 85). Likewise, it was demonstrated that SIDT2 functions in the endolysosomal transport of dsRNA from different dsRNA-producing viruses in the initiation of the innate immune response, which is impaired in Sidt2 (–/–) knockout mice (24). Most significantly, a recent report has demonstrated that levels of SIDT2 strongly correlate with those of alpha-synuclein, both of which are increased, in the postmortem brains of patients with PD and dementia with Lewy bodies (26). Therefore, the descriptive pathology of human synucleinopathies mirror our functional observations in *C. elegans*; both suggesting that the downregulation of dsRNA transport may be protective to dopaminergic neurons under conditions of neurotoxic stress. Clearly, mammalian correlates to the dual-transporter regulatory integration we have revealed may take on an evolutionarily divergent form, and this necessitates further experimentation.

All prior research on SID-3 has focused on its established function in *C. elegans* as a mediator of dsRNA uptake and RNAi silencing in the somatic cells through its regulation of the dsRNA transporter, SID-1 (18). Since *C. elegans* dopaminergic neurons have proven refractory to RNAi in wild-type animals, presumably due to lower levels of SID-1 expression, it was therefore important to clarify whether dsRNA silencing activity was preserved in these cells. Others and we have previously demonstrated that targeted overexpression of *sid-1* in worm neurons, as well as selectively in neuronal subtypes using different promoters, confers enhanced sensitivity to RNAi knockdown by exogenous bacterial feeding of dsRNA (31, 86, 87). Thus, the basic cellular machinery for RNAi is not completely absent from these neurons. It follows that endogenous *sid-1* expression in the dopaminergic neurons was confirmed through the recently completed the *C. elegans* neuronal transcriptome (88).

We found that *sid-1(pk3321)* mutant animals displayed significantly less 6-OHDA-induced neurodegeneration when compared with wild-type worms, but this effect was not as strong as was observed with *sid-3(ok973)* mutants (Fig. 3*C*). This is both an interesting and logical result. We demonstrated that *sid-3(ok973)* mutants exhibited neuroprotection from 6-OHDA uptake, as a measure of DAT-1 endocytosis (Fig. 1 *A*, *B*, and *E*). Similarly, we also established that SID-3 modulates RNAi silencing in the dopaminergic neurons, a readout reflective of the endocytic regulation of SID-1 (Fig. 3 *A* and *B*). Thus, the observed neuroprotection in *sid-1(pk3321*) mutants would be expected to be due to a lack of dsRNA import, preventing the silencing of genes involved in pathways required to maintain dopamine homeostasis. In contrast, the enhanced level of protection observed in the *sid-3(ok973)* animals reflects the additive effect that loss of SID-3 function exerts in the coregulation of DAT-1. We further demonstrate that this regulatory intersection can be modulated pharmacologically, through AIM-100 exposures that inhibit the activity of SID-3/TNK2 to impede RNAi silencing, in addition to conferring neuroprotection in vivo. Notably, AIM-100 treatments and CRISPR-knockouts of *TNK2* have also been shown to prevent viral infection in human cell cultures (20). These combined findings strongly support a conserved functional role for TNK2 as a modulator of dsRNA and illustrate its potential as a druggable target.

The chemical-genetic approach employed here highlights the utility of *C. elegans* models in parsing out the intricacies of cellular mechanisms. This strategy represents an effective means for more rapid, costeffective, and functionally justified prioritization of therapeutic targets for preclinical research in neurodegenerative diseases (89). This is borne out by the observed specificity of NAB2 as an effector of only the dopaminergic regulatory contribution to the neuroprotection and illustrates a subtle but significant difference exists in the endocytic regulation of dopamine compared with dsRNA transport. We speculate that SID-3 may bind to either DAT-1 or SID-1 through alternative motifs; when bound to SID-1, the activated NEDD4/WWP-1 E3 ligase may be unable to interact with TNK2/SID-3 to target it for degradation. This is supported by evidence that the NCK-1/SID-4 protein, a SH2/SH3 domain-containing adaptor protein, is also required for SID-3-dependent RNAi silencing (90). Thus, a putative complex between SID-3 and NCK-1/SID-4 may represent a steric hinderance to NEDD4/WWP-1 interaction. Further investigation is needed to discern an underlying cause for this mechanistic distinction.

Last, we sought to provide functional clarity by evaluating the identified PD-related SNPs in *TNK2* (1). Using CRISPR technology, two of these mutations that coded for missense mutations in conserved regions of SID-3 were engineered and the modified animals were assayed for 6-OHDA neurotoxicity and RNAi-targeted knockdown of GFP in dopaminergic neurons. Animals expressing either of the two SNP variants exhibited increased sensitivity to 6-OHDA exposures (Fig. 4*C*). Furthermore, our analyses on the CRISPR-edited animals using either NAB2 or AIM-100 treatment highlighted the pathological importance these variants. The UBA-domain SNP abolished NAB2-protection from 6-OHDA (Fig. 4*E*), whereas animals with the PKD-localized SNP retained neuroprotection with AIM-100 (Fig. 4*F*). This latter result is consistent with what has been shown in human cell cultures where AIM-100 prevented the increased phosphorylation of a TNK2 variant harboring a similar SNP in the same domain (91). Importantly, neither of these SNPs exerted a discernable change in dopaminergic neuronal RNAi silencing (Fig. 4*D*), indicating that SID-3 retained its functional effect on dsRNA import in *C. elegans*. Given that these PD-specific variants appear to encode either a degradation-resistant or hyperactive enzyme, these would not be expected to diminish dsRNA-dependent silencing, as was observed with a *sid-3* knockout mutant (that defines "systemic RNAi deficiency"). Thus, the pathological consequences of this interplay may be significant, and synergistic, to effects on DA dysregulation, considering that we have shown neuroprotection from 6-OHDA is at least partially an outcome of reduced gene silencing.

Our results highlight the functional significance of both NEDD4 and TNK2, and how their interaction plays a vital role in modulating presynaptic neuroplasticity (Fig. 5). Future studies, ideally using *TNK2* patient-derived neurons from iPSCs, would be informative when considering NAB2 was already proven efficacious in conferring neuroprotection to PD-patient-derived dopaminergic neurons in culture (8). Efforts directed at investigating the remaining two discovered SNPs in *TNK2* are likely to provide further insights (1). Characterization of a mutation in TNK2 (R877H) adjacent to the epidermal growth factor receptor-binding domain (EBD; Fig. 4*A*) might be expected to result in a gain-of-function phenotype, since TNK2 phosphorylation was shown to be stimulated by EGFR-ligand binding (91). The other remaining SNP, located in the putative NEDD4-binding

motif of TNK2 (Fig. 4*A*; V638M), also warrants attention, given our results with the UBA-localized mutation, and since a similar SNP found in epilepsy patients was reported to block NEDD4-TNK2 interaction (52). Our findings using rat primary neurons (Fig. 2), where NAB2 treatment caused a reduction in TNK2 protein levels, in addition to resistance to 6-OHDA neurotoxicity, speak to the translational significance of the interaction between NEDD4 and TNK2 in mammals. This study provides a perspective through which to consider gene-by-environment interactions in PD. In this regard, we recently reported that overexpression of an established genetic modifier of DA neuron degeneration, human alpha-synuclein, in transgenic *C. elegans* is attenuated by loss of SID-1 or SID-3 function (92). Furthermore, we uncovered a series of genes, all with human homologs, that are suppressed by import of a specific miRNA via SID-1/SID-3 into DA neurons. Knockout or inhibition of SID-3 with AIM-100 released suppression and resulted in robust neuroprotection. Extending this work with other genetic contributors to PD (i.e., *LRRK2*, *GBA1*) represents an untapped source of potential therapeutic targets that can be unmasked using *C. elegans*.

The optimal function and survival of dopaminergic neurons is a consequence of a variety of intrinsic factors (genetics, proteostasis, aging, oxidative stress, mitochondrial/lysosomal function), all of which combine to modulate brain activity. Given the scale and diversity of dopamine-associated disorders, one would not be incorrect to assume these factors seemingly act near a precipice of dysfunction—yet are poised for response to epigenetic influences that raise or lower this threshold. The evolution of integrated cellular mechanisms in the intricate management of dopaminergic neuron health to provide for a capacity to respond, adapt, and buffer neurons, to and from external stressors, exemplifies the delicate balance between resilience or susceptibility—and, at times, life or death.

Materials and Methods

***C. elegans* 6-OHDA Neurodegeneration Assays.** Animals were scored for 6-OHDA-induced neurodegeneration as previously described (39, 40). Briefly, worm strains were synchronized at hatching and raised on agar plates of Nematode Growth Media (NGM) seeded with *Escherichia coli* strain OP-50 at 20 °C. L4-stage larvae were collected from plates by resuspension using ddH_2O and transferred to 10-mL glass conical tubes, centrifuged, and then washed thrice with ddH_2O to remove bacteria. Animals were subsequently transferred to a 1.5-mL Lo-Bind tube and treated with 6-OHDA (Tocris) containing 2 mM ascorbic acid for 1-h, while rotating at 20 °C. After 1-h incubation with 6-OHDA, M9 was added to oxidize 6-OHDA and terminate the experiment. Worms were immediately washed thrice with ddH_2O or until the supernatant was no longer pink (indicative of oxidation). Washed worms were placed onto freshly seeded plates and scored for neurodegeneration 24 h later. The six anterior dopaminergic neurons of *C. elegans* were scored in each animal as previously described (38, 39). Briefly, worms were scored under a fluorescent microscope using the 60× objective. Animals were scored as "normal" if no degenerative phenotypes (dendritic blebbing, swollen or shrunken soma, broken projections, or a missing neuron) in the six anterior [four CEPs (cephalic) and two ADEs (anterior deirid)] DA neurons. Three trials consisting of 30 animals per replicate, totaling to 90 animals/strain/condition.

AIM-100 and NAB2 Drug Treatments in Neurodegeneration Assays. Stocks of AIM-100 and NAB2 (Tocris) were dissolved in 200 proof ethanol and kept at 4 °C. Synchronized *C. elegans* were treated daily with either drug. For drug exposure, worms were resuspended from OP-50 plates with ddH_2O, transferred to a 10-mL glass conical tube, and washed thrice with 10 mL ddH_2O to remove bacteria. Worms were then transferred to a fresh 1.5-mL Lo-Bind tube and suspended in 100 μM concentration of AIM-100, NAB2, or 0.01% ethanol diluted in 0.5× M9. 1.5-mL Lo-Bind tubes of worms, and drugs were kept rotating at 20 °C for 1-h. After exposure, drugs were washed away 3 times with ddH_2O, and worms were placed onto fresh OP-50 plates, then maintained at 20 °C. On days of 6-OHDA treatments, worms treated with either AIM-100 or NAB2, as described, transferred to a fresh 1.5-mL Lo-Bind tube after washout of drugs, then immediately exposed to 6-OHDA. Animals were scored for neurodegeneration 24 h later.

***C. elegans* RNAi.** The GFP RNAi construct was plasmid L4417, a gift from Andrew Fire (Addgene plasmid #1649). Bacteria were isolated and grown overnight at 37 °C shaking in Luria broth containing 100 μg/mL ampicillin. NGM plates containing 50 μg/mL ampicillin and 1 mM IPTG were seeded with 300 μL RNAi bacterial culture and allowed to dry and grow overnight at 20 °C under foil. Animals were raised on RNAi bacteria for two generations and scored for dopaminergic GFP silencing at day 5 posthatching in the second generation. The six anterior dopaminergic neurons were scored under a fluorescent microscope using a 60× objective. If all six anterior neurons were visible, then the animal was scored as normal, while if any of the neurons were not visible (i.e., nonfluorescent) then the animal was scored as abnormal.

Swimming-induced Paralysis Assays. SWIP analysis was performed as previously described (43). Briefly, 10 to 15 worms, synchronized to the L4 stage, were placed into well containing 200 μL water and allowed to thrash for 10 min. After 10 min, the wells were observed by eye under a dissecting scope, and the number of animals still moving were recorded. Ten wells were scored for each strain. Significance was determined by one-way ANOVA with Dunnett's post hoc test.

***C. elegans* Strains.** Worms were grown on plates containing standard Nematode Growth Medium (NGM) that were seeded with *Escherichia coli* strain OP-50 bacterial lawns. All strains were maintained at 20 °C under standard laboratory conditions (93). Strains used in this study include: N2 (Bristol; "wildtype"), NL3321 (*sid-1(pk3321)*), VC787 (*sid-3(ok973)*), RM2702 *(dat-1(ok157))*, GR1373 (*eri-1(mg366)*), VC889 *(wwp-1(gk372))*, PHX898 *(sid-3(syb898))*, PHX912 *(sid-3(syb912)*, and BY250 (*vtIs7*[P_{dat-1}::GFP]; kindly provided by Randy Blakely). Crosses performed to generate strains used in this study are in Table 1. Briefly, BY250 was crossed separately into NL3321, VC787, RM2702, GR1373, VC889, PHX898 and PHX912 to create UA423, UA424, UA407, UA425, UA426, UA427 and UA428, respectively (Table 1). The resulting cross of UA425 was further crossed separately into both PHX898 and PHX912 to create UA429 and UA430, respectively (Table 1). Genome editing of *C. elegans* (wildtype, N2) was performed to generate the *sid-3(syb898) and sid-3(syb912)* mutant alleles, strains PHX898 and PHX912, respectively, using CRISPR by SunyBiotech (Fujian, China), as detailed in *SI Appendix*. Animals with the specified mutant alleles were verified by Sanger sequencing, both by the company and independently by us, following outcrossing.

Culture of Primary Neurons. Primary rat cortical and dopaminergic neurons were prepared from rat feti (Sprague–Dawley, day 18 of gestation; Envigo, Indianapolis, IN) as described previously (94). Briefly, neurons (0.5×10^6 cells/ 35 mm plate) were grown in neurobasal medium supplemented with B-27, glutamine, and antibiotics (Thermo Fisher Scientific, Waltham, MA, USA) for 12 d in vitro. NAB2 treatment: A solution of NAB2 (Tocris) was prepared in filter-sterilized 99.9% DMSO (Sigma-Aldrich, St. Louis, MO, USA) and added to the cell culture medium (final concentration: 2 mM) for 24 h, at which point they were analyzed. The vehicle control group was treated with isovolumetric sterile DMSO. 6-OHDA treatment: 6-OHDA (20 μM) was prepared in sterile water and added to the cell culture medium. The stock solution of 6-OHDA was prepared in ascorbic acid (final concentration 4 μM). The vehicle control group for 6-OHDA was treated with isovolumic sterile water. Cells were treated for 24 h and then immediately analyzed. All protocols were approved by the Institutional Animal Care Committee of The University of Alabama.

Immunoblots. After treatment with or without NAB2 for 24 h, cortical neurons were scraped and lysed in 1× cell signaling buffer (Cell Signaling Technology, Danvers, MA, USA) and protein concentration was determined using the BCA protein assay (Thermo Fisher Scientific, Waltham, MA, USA). Samples (50 μg protein/lane) were separated on a 4 to 12% SDS-polyacrylamide gel (Bio-Rad, Hercules, CA, USA) and probed with anti-ACK1 antibody (1:100, Santa Cruz, Dallas, TX, USA) and anti-β-actin (1:1,000, Sigma-Aldrich, St. Louis, MO, USA). Scanned images were analyzed using ImageJ software (NIH, Bethesda, MD, USA).

Table 1. Completed crosses for strains used

Strain	Genotype	Strains Crossed
UA407	*dat-1(ok157); vtIs7*[P_{dat-1}::GFP]	RM2702 × BY250
UA423	*sid-1(pk3321); vtIs7*[P_{dat-1}::GFP]	NL3321 × BY250
UA424	*sid-3(ok973); vtIs7*[P_{dat-1}::GFP]	VC787 × BY250
UA425	*eri-1(mg366); vtIs7*[P_{dat-1}::GFP]	GR1373 × BY250
UA426	*wwp-1(gk372); vtIs7*[P_{dat-1}::GFP]	VC889 × BY250
UA427	*sid-3(syb898); vtIs7*[P_{dat-1}::GFP]	PHX898 (SID-3 I341A) × BY250
UA428	*sid-3(syb912); vtIs7*[P_{dat-1}::GFP]	PHX912 (SID-3 A1016V) × BY250
UA429	*sid-3(syb898); eri-1(mg366); vtIs7*[P_{dat-1}::GFP]	PHX898 (SID-3 I341A) × UA425
UA430	*sid-3(syb912); eri-1(mg366); vtIs7*[P_{dat-1}::GFP]	PHX912 (SID-3 A1016V) × UA425

Immunocytochemistry. Primary dopaminergic neurons fixed in 10% buffered formalin were blocked in 10% goat serum for 1 h, then incubated with anti-TH antibody (1:100, Pelfreez-Bio, Rogers, AR, USA) overnight at 4 °C. Cells were washed and incubated with Alexa-568 antibody (1:200 dilution; Invitrogen, Molecular Probes, Carlsbad, CA, USA) for 1 h at room temperature. Images were taken with a Zeiss Axiovert A1 microscope. Neurons were classified into two different categories: live group, TH+ cells with neurites presenting polarity and arborization; dead group, TH+ cells with a small round nucleus, a shrunken cytoplasm, and degraded or absence of neurites. TH+ live cells and TH+ dead cells were counted using AxioVision 4.9.; percentage of viable dopaminergic neurons was calculated using the following equation: Viable TH+ cells (%) = the number of TH+ and DAPI-positive live cell / (TH+ and DAPI-positive live cells + TH+ and DAPI-positive dead cells) × 100.

Data, Materials, and Software Availability. All study data are included in the article and/or *SI Appendix*.

ACKNOWLEDGMENTS. We wish to acknowledge all members of The Caldwell Lab for their teamwork, with special thanks for the technical assistance from Adam Holzhauer and Brian Smithers, and the expert advice of Laura Berkowitz. We are especially grateful to Anthony Gaeta, Ed Griffin, Jennie Thies, and Xiaohui Yan for their scientific insights. We wish to thank Wormbase, as well as Randy Blakely and Andrew Fire for strains and vectors. This research was funded by a grant to Guy A. Caldwell from the US Department of Health & Human Services, National Institute of Neurological Disorders and Stroke (R15NS104857). Some strains were provided by the CGC, funded by NIH Office of Research Infrastructure Programs (P40 OD010440); other support came from The University of Alabama College of Arts & Sciences, The Hill Crest Foundation, and the Parkinson's Disease Support Group of Huntsville, Alabama.

Author affiliations: [a]Department of Biological Sciences, The University of Alabama, Tuscaloosa, AL 35487; [b]Department of Human Nutrition and Hospitality Management, The University of Alabama, Tuscaloosa, AL 35487; [c]Alabama Research Institute on Aging, The University of Alabama, Tuscaloosa, AL 35487; [d]Center for Convergent Bioscience and Medicine, The University of Alabama, Tuscaloosa, AL 35487; and [e]Department of Neurology, Center for Neurodegeneration and Experimental Therapeutics, Nathan Shock Center of Excellence for Research in the Basic Biology of Aging, Heersink School of Medicine, University of Alabama at Birmingham, Birmingham, AL 35294

1. J. L. Farlow *et al.*, Whole-exome sequencing in familial Parkinson disease. *JAMA Neurol.* **73**, 68–75 (2016).
2. J. M. Ureña *et al.*, Expression, synaptic localization, and developmental regulation of Ack1/Pyk1, a cytoplasmic tyrosine kinase highly expressed in the developing and adult brain. *J. Compar. Neurol.* **490**, 119–132 (2005).
3. M. Fox, C. Crafter, D. Owen, The non-receptor tyrosine kinase ACK: Regulatory mechanisms, signaling pathways and opportunities for attacking cancer. *Biochem. Society Transact.* **47**, 1715–1731 (2019).
4. S. Wu, K. D. Bellve, K. E. Fogarty, H. E. Melikian, Ack1 is a dopamine transporter endocytic brake that rescues a trafficking-dysregulated ADHD coding variant. *Proc. Natl. Acad. Sci. U.S.A.* **112**, 15480–15485 (2015).
5. M. Teo, L. Tan, L. Lim, E. Manser, The tyrosine kinase ACK1 associates with clathrin-coated vesicles through a binding motif shared by arrestin and other adaptors. *J. Biol. Chem.* **276**, 18392–18398 (2001).
6. Q. Lin *et al.*, HECT E3 ubiquitin ligase Nedd4-1 ubiquitinates ACK and regulates epidermal growth factor (EGF)-induced degradation of EGF receptor and ACK. *Molec. Cell. Biol.* **30**, 1541–1554 (2010).
7. R. R. Fagan *et al.*, Dopamine transporter trafficking and Rit2 GTPase: Mechanism of action and *in vivo* impact. *J. Biol. Chem.* **295**, 5229–5244 (2020).
8. C. Y. Chung *et al.*, Identification and rescue of α-synuclein toxicity in Parkinson patient–derived neurons. *Science* **342**, 983–987 (2013).
9. D. F. Tardiff *et al.*, Yeast reveal a druggable Rsp5/Nedd4 network that ameliorates α-synuclein toxicity in neurons. *Science* **342**, 979–983 (2013).
10. J. A. Conway, G. Kinsman, E. R. Kramer, The role of NEDD4 E3 ubiquitin-protein ligases in Parkinson's disease. *Genes* **13**, 513 (2022).
11. C. D. Cristobal *et al.*, Daam2 regulates myelin structure and the oligodendrocyte actin cytoskeleton through Rac1 and Gelsolin. *J. Neurosci.* **42**, 1679–1691 (2022).
12. E. M. Rodrigues, S. L. Scudder, M. S. Goo, G. N. Patrick, Aβ-induced synaptic alterations require the E3 ubiquitin ligase Nedd4-1. *J. Neurosci.* **36**, 1590–1595 (2022).
13. E. Y. Yuen *et al.*, Repeated stress causes cognitive impairment by suppressing glutamate receptor expression and function in the prefrontal cortex. *Neuron* **73**, 962–977 (2012).
14. G. Sanacora, Y. Zhen, M. Popoli, The stressed synapse 2.0.: Pathological mechanisms in stress-related neuropsychiatric disorders. *Nat. Rev. Neurosci.* **23**, 86–103 (2022).
15. G. K. Chen *et al.*, Stochastic epigenetic mutations influence Parkinson's disease risk, progress, and mortality. *J. Parkinson Dis.* **12**, 545–556 (2022).
16. F. J. S. Lee, F. Liu, Z. B. Pristupa, H. B. Niznik, Direct binding and functional coupling of α-synuclein to the dopamine transporters accelerate dopamine-induced apoptosis. *FASEB J.* **15**, 916–926 (2001).
17. D. E. Mor *et al.*, Dopamine induces soluble α-synuclein oligomers and nigrostriatal degeneration *Nat. Neurosci.* **20**, 1560–1568 (2017).
18. A. M. Jose, Y. A. Kim, S. Leal-Ekman, C. P. Hunter, Conserved tyrosine kinase promotes the import of silencing RNA into *Caenorhabditis elegans* cells. *Proc. Natl. Acad. Sci. U.S.A.* **109**, 14520–14525 (2012).
19. H. Jiang, K. Chen, L. E. Sandoval, C. Leung, D. Wang, An evolutionarily conserved pathway essential for Orsay virus infection of *Caenorhabditis elegans*. *mBio* **8**, e00940-17 (2017).
20. H. Jiang, C. Leung, S. Tahan, D. Wang, Entry by multiple picornaviruses is dependent on a pathway that includes TNK2. *WASL, and NCK1. eLife* **8**, e5027 (2019).
21. W. M. Winston, C. Molodowitch, C. P. Hunter, Systemic RNAi in *Caenorhabditis elegans* requires the putative transmembrane protein SID-1. *Science* **295**, 2456–2459 (2022).
22. K. Cappelle, C. F. R. de Oliveira, B. Van Eynde, O. Christiaens, G. Smagghe, The involvement of clathrin-mediated endocytosis and two Sid-1-like transmembrane proteins in double-stranded RNA uptake in the Colorado potato beetle midgut. *Insect Molec. Biol.* **25**, 315–323 (2016).
23. M. O. Elhassan, J. Christie, M. S. Duxbury, *Homo sapiens* Systemic RNA Interference-defective-1 transmembrane family member 1 (SIDT1) protein mediates contact-dependent small RNA transfer and microRNA-21-driven chemoresistance. *J. Biol. Chem.* **287**, 5267–5277 (2012).
24. T. A. Nguyen *et al.*, SIDT2 transports extracellular dsRNA into the cytoplasm for innate immune recognition. *Immunity* **47**, 498–509 (2017).
25. T. A. Nguyen *et al.*, SIDT1 localizes to endolysosomes and mediates double-stranded RNA transport into the cytoplasm. *J. Immunol.* **202**, 3483–3492 (2019).
26. Y. Fujiwara *et al.*, Pathology-associated change in levels and localization of SIDT2 in postmortem brains of Parkinson's disease and dementia with Lewy bodies patients. *Neurochem. Intl.* **152**, 105243 (2022).
27. A. A. Cooper *et al.*, α-Synuclein blocks ER-Golgi traffic and Rab1 rescues neuron loss in Parkinson's models. *Science* **313**, 324–328 (2006).
28. A. D. Gitler *et al.*, The Parkinson's disease protein alpha-synuclein disrupts cellular Rab homeostasis. *Proc. Natl. Acad. Sci. U.S.A.* **105**, 145–150 (2008).
29. S. Hamamichi *et al.*, Hypothesis-based RNAi screening identifies neuroprotective genes in a Parkinson's disease model. *Proc. Natl. Acad. Sci. U.S.A.* **105**, 728–733 (2008).
30. J. R. Mazzulli *et al.*, Gaucher's disease glucocerebrosidase and α-synuclein form a bidirectional pathogenic loop in synucleinopathies. *Cell* **146**, 37–52 (2011).
31. A. J. Harrington, T. A. Yacoubian, S. R. Sloane, K. A. Caldwell, G. A. Caldwell, Functional analysis of VPS41-mediated neuroprotection in *Caenorhabditis elegans* and mammalian models of Parkinson's disease. *J. Neurosci.* **32**, 2142–2153 (2012).
32. A. L. Knight *et al.*, The glycolytic enzyme, GPI, is a functionally conserved modifier of dopaminergic neurodegeneration in Parkinson's models. *Cell Metab.* **20**, 145–157 (2014).
33. A. Ray, S. Zhang, C. Rentas, K. A. Caldwell, G. A. Caldwell, RTCB-1 mediates neuroprotection via XBP-1 mRNA splicing in the unfolded protein response pathway. *J. Neurosci.* **34**, 16076–16085 (2014).
34. B. A. Martinez *et al.*, Dysregulation of the mitochondrial unfolded protein response induces non-apoptotic dopaminergic neurodegeneration in *Caenorhabditis elegans* models of Parkinson's disease. *J. Neurosci.* **37**, 11085–11100 (2017).

35. S. Zhang, S. A. Glukhova, K. A. Caldwell, G. A. Caldwell, NCEH-1 modulates cholesterol metabolism and protects against a-synuclein toxicity in a *Caenorhabditis elegans* model of Parkinson's disease *Hum. Mol. Genet.* **26**, 3823–3836 (2017).
36. E. F. Griffin *et al.*, Distinct functional roles of Vps41-mediated neuroprotection in Alzheimer's and Parkinson's disease models of neurodegeneration. *Hum. Mol. Genet.* **27**, 4176–4193 (2018).
37. R. E. N. van der Welle *et al.*, Neurodegenerative VPS41 variants inhibit HOPS function and mTORC1-dependent TFEB/TFE3 regulation. *EMBO Molec. Med.* **13**, e13258 (2021).
38. A. J. Harrington, A. L. Knight, G. A. Caldwell, K. A. Caldwell, *Caenorhabditis elegans* as a model system for identifying effectors of α-synuclein misfolding and dopaminergic cell death associated with Parkinson's disease. *Methods* **53**, 220–225 (2011).
39. L. A. Berkowitz *et al.*, Application of a *Caenorhabditis elegans* dopamine neuron degeneration assay for the validation of potential Parkinson's disease genes. *J. Vis. Exp.* **17**, 835 (2008).
40. R. Nass, D. H. Hall, D. M. Miller, R. D. Blakely, Neurotoxin-induced degeneration of dopamine neurons in Caenorhabditis elegans. *Proc. Natl. Acad. Sci. U.S.A.* **99**, 3264–3269 (2002).
41. E. F. DiMauro *et al.*, Discovery of 4-amino-5, 6-biaryl-furo [2, 3-d] pyrimidines as inhibitors of Lck: development of an expedient and divergent synthetic route and preliminary SAR. *Bioorg. Med. Chem. Lett.* **17**, 2305–2309 (2007).
42. K. Mahajan *et al.*, Effect of Ack1 tyrosine kinase inhibitor on ligand-independent androgen receptor activity. *Prostate* **70**, 1274–1285 (2010).
43. P. W. McDonald *et al.*, Vigorous motor activity in *Caenorhabditis elegans* requires efficient clearance of dopamine mediated by synaptic localization of the dopamine transporter DAT-1. *J. Neurosci.* **27**, 14216–14227 (2007).
44. H. E. Melikian, K. M. Buckley, Membrane trafficking regulates the activity of the human dopamine transporter. *J. Neurosci.* **19**, 7699–7710 (1999).
45. W. Chan *et al.*, Down-regulation of active ACK1 is mediated by association with the E3 ubiquitin ligase Nedd4-2. *J. Biol. Chem.* **284**, 8185–8194 (2009).
46. G. K. Tofaris *et al.*, Ubiquitin ligase Nedd4 promotes α-synuclein degradation by the endosomal-lysosomal pathway. *Proc. Natl. Acad. Sci. U.S.A.* **108**, 17004–17009 (2011).
47. J. W. Astin, N. J. O'Neil, P. Kuwahara, Nucleotide excision repair and the degradation of RNA pol II by the Caenorhabditis elegans XPA and Rsp5 orthologues, RAD-3 and WWP-1. *DNA Repair (Amst)* **7**, 267–280 (2008).
48. T. W. Peters *et al.*, Natural genetic variation in yeast reveals that NEDD4 is a conserved modifier of mutant polyglutamine aggregation. *G3(Bethesda)* **8**, 3421–3431 (2018).
49. S. Asikainen, S. Vartiainen, M. Lakso, R. Nass, G. Wong, Selective sensitivity of *Caenorhabditis elegans* neurons to RNA interference. *NeuroReport* **16**, 1995–1999 (2005).
50. S. Kennedy, D. Wang, G. Ruvkun, A conserved siRNA-degrading RNase negatively regulates RNA interference in *Caenorhabditis elegans*. *Nature* **427**, 645–649 (2004).
51. K. Mahajan, N. P. Mahajan, ACK1/TNK2 tyrosine kinase: molecular signaling and evolving role in cancers. *Oncogene* **34**, 4162–4167 (2015).
52. Y. Hitomi *et al.*, Mutations in TNK2 in severe autosomal recessive infantile onset epilepsy. *Ann. Neurol.* **74**, 496–501 (2013).
53. T.-Y. Chan *et al.*, TNK1 is a ubiquitin-binding and 14-3-3-regulated kinase that can be targeted to block tumor growth. *Nat. Comm.* **12**, 5537 (2021).
54. J. N. Cochran *et al.*, Genome sequencing for early-onset or atypical dementia: high diagnostic yield and frequent observation of multiple contributory alleles. *Cold Spring Harb. Mol. Case Stud.* **5**, a003491 (2019).
55. G. Pagano, N. Ferrara, D. J. Brooks, N. Pavese, Age at onset and Parkinson's disease phenotype. *Neurology* **86**, 1400–1407 (2016).
56. R. B. Ramoni *et al.*, The undiagnosed diseases network: Accelerating discovery about health and disease. *Am. J. Hum. Genet.* **100**, 185–192 (2017).
57. P. A. Kropp, B. Rosemary, I. Zafra, C. Graham, A. Golden, *Caenorhabditis elegans* for rare disease modeling and drug discovery: strategies and strengths *Dis. Model. Mech.* **14**, dmm049010 (2021).
58. J.-H. Lee, Invertebrate model organisms as a platform to investigate rare human neurological diseases. *Exp. Neurobiol.* **31**, 1–16 (2022).
59. M. Ma, M. J. Moulton, S. Lu, H. J. Bellen, Fly-ing' from rare to common neurodegenerative disease mechanisms. *Trends Genet.* **38**, 972–984 (2022).
60. J.-F. Guo *et al.*, Coding mutations in *NUS1* contribute to Parkinson's disease. *Proc. Natl. Acad. Sci. U.S.A.* **115**, 11567–11572 (2018).
61. E. Bangi *et al.*, A personalized platform identifies trametinib plus zoledronate for a patient with KRAS-mutant metastatic colorectal cancer. *Sci. Adv.* **5**, eaav6528 (2019).
62. E. Bangi *et al.*, A Drosophila platform identifies a novel, personalized therapy for a patient with adenoid cystic carcinoma. *iScience* **24**, 102212 (2021).
63. T. A. McDiarmid *et al.*, Systematic phenomics analysis of autism-associated genes reveals parallel networks underlying reversible impairments in habituation. *Proc. Natl. Acad. Sci. U.S.A.* **117**, 656–67 (2020).
64. A. Berson, R. Nativio, S. L. Berger, N. M. Bonini, Epigenetic regulation in neurodegenerative diseases. *Trends Neurosci.* **41**, 587–598 (2018).
65. R. Nativio *et al.*, An integrated multi-omics approach identifies epigenetic alterations associated with Alzheimer's disease. *Nat. Genet.* **52**, 1024–1035 (2020).
66. M. Mew, K. A. Caldwell, G. A. Caldwell, From bugs to bedside: functional annotation of human genetic variation for neurological disorders using invertebrate models. *Hum. Mol. Genet.* **31**, R37–R46 (2022).
67. D. Stajic, L. E. T. Jansen, Empirical evidence for epigenetic inheritance driving evolutionary adaptation. *Philos. Trans. R. Soc. Lond. B. Biol. Sci.* **376**, 20200121 (2021).
68. D. Gentilini *et al.*, Stochastic epigenetic mutations (DNA methylation) increase exponentially in human aging and correlate with X chromosome inactivation skewing in females. *Aging* **7**, 568–78 (2015).
69. J. M. Shulman *et al.*, Functional screening of Alzheimer pathology genome-wide association signals in Drosophila. *Am. J. Hum. Genet.* **88**, 232–238 (2011).
70. L. McGurk, A. Berson, N. M. Bonini, Drosophila as an *in vivo* model for human neurodegenerative disease. *Genetics* **201**, 377–402 (2015).
71. A. L. Gaeta, K. A. Caldwell, G. A. Caldwell, Found in translation: The utility of *Caenorhabditis elegans* alpha-synuclein models of Parkinson's disease. *Brain Sci.* **9**, 73 (2019).
72. S. L. Ameres, P. D. Zamore, Diversifying microRNA sequence and function. *Nat. Rev. Molec. Cell. Biol.* **4**, 475–88 (2013).
73. R. C. Lee, R. L. Feinbaum, V. Ambros, The *Caenorhabditis elegans* heterochronic gene *lin-4* encodes small RNAs with antisense complementarity to *lin-14*. *Cell* **75**, 843–854 (1993).
74. B. Wightman, I. Ha, G. Ruvkun, Posttranscriptional regulation of the heterochronic gene *lin-14* by *lin-4* mediates temporal pattern formation in *Caenorhabditis elegans*. *Cell* **75**, 855–862 (1993).
75. A. Fire *et al.*, Potent and specific genetic interference by double-stranded RNA in *Caenorhabditis elegans*. *Nature* **391**, 806–811 (1998).
76. E. H. Feinberg, C. P. Hunter, Transport of dsRNA into cells by the transmembrane protein SID-1. *Science* **301**, 1545–1547 (2003).
77. J. D. Shih, C. P. Hunter, SID-1 is a dsRNA-selective dsRNA-gated channel. *RNA* **17**, 1057–1065 (2011).
78. S. Aizawa *et al.*, Lysosomal putative RNA transporter SIDT2 mediates direct uptake of RNA by lysosomes. *Autophagy* **12**, 565–578 (2016).
79. Q. Chen *et al.*, SIDT1-dependent absorption in the stomach mediates host uptake of dietary and orally administered microRNAs. *Cell Res.* **31**, 247–258 (2021).
80. G. Jialin, G. Xuefan, Z. Huiwen, SID1 transmembrane family, member 2 (Sidt2): a novel lysosomal membrane protein. *Biochem. Biophys. Res. Commun.* **402**, 588–594 (2010).
81. J. Gao, X. Gu, D. J. Mahuran, Z. Wang, H. Zhang, Impaired glucose tolerance in a mouse model of sidt2 deficiency. *PLoS One* **8**, e66139 (2013).
82. V. J. Valdes, A. Athie, L. S. Salinas, R. E. Navarro, L. Vaca, CUP-1 is a novel protein involved in dietary cholesterol uptake in *Caenorhabditis elegans*. *PloS One* **7**, e33962 (2012).
83. K. M. Méndez-Acevedo, V. J. Valdes, A. Asanov, L. Vaca, A novel family of mammalian transmembrane proteins involved in cholesterol transport *Sci. Rep.* **7**, 7450 (2017).
84. J. S. Whangbo, A. S. Weisman, J. Chae, C. P. Hunter, SID-1 domains important for dsRNA import in *Caenorhabditis elegans*. *G3(Bethesda)* **7**, 3887–3899 (2017).
85. B. Otarigo, A. Aballay, Cholesterol regulates innate immunity via nuclear hormone receptor NHR-8. *iScience* **23**, 101068 (2020).
86. A. Calixto, D. Chelur, I. Topalidou, X. Chen, M. Chalfie, Enhanced neuronal RNAi in *Caenorhabditis elegans* using SID-1. *Nat. Methods* **7**, 554–559 (2010).
87. S. Treusch *et al.*, Functional links between Aβ toxicity, endocytic trafficking, and Alzheimer's disease risk factors in yeast. *Science* **334**, 1241–1245 (2011).
88. S. R. Taylor *et al.*, Molecular topography of an entire nervous system. *Cell* **184**, 4329–4347 (2021).
89. K. A. Caldwell, C. W. Willicott, G. A. Caldwell, Modeling neurodegeneration in *Caenorhabditis elegans Dis. Model. Mech.* **13**, dmm046110 (2020).
90. S. Bhatia, C. P. Hunter, SID-4/NCK-1 is important for dsRNA import in *Caenorhabditis elegans*. *G3* **12**, jkac252 (2022).
91. K. Mahajan *et al.*, Ack1 mediated AKT/PKB tyrosine 176 phosphorylation regulates its activation. *PLoS One* **5**, e9646 (2010).
92. A. L. Gaeta *et al.*, Systemic RNA interference defective (SID) genes modulate dopaminergic neurodegeneration in *Caenorhabditis elegans*. *PLoS Genet.* **18**, e1010115 (2022).
93. S. Brenner, The genetics of *Caenorhabditis elegans*. *Genetics* **77**, 71–94 (1974).
94. H-A. Park *et al.*, Role of lycopene in mitochondrial protection during differential levels of oxidative stress in primary cortical neurons. *Brain Disord.* **3**, 100016 (2021).